Solid Earth Discuss., https://doi.org/10.5194/se-2018-8
Manuscript under review for journal Solid Earth
Discussion started: 7 February 2018

Solid Earth Discussions
Open Access
EGU

The long-term GIA signal at present-day in Scandinavia, northern Europe and the British Isles estimated from GPS and GRACE data

Karen M. Simon[1*], Riccardo E.M. Riva[1], Marcel Kleinherenbrink[1], Thomas Frederikse[1,2]

[1]Delft University of Technology, Department of Geoscience and Remote Sensing, Stevinweg 1, 2628 CN Delft, the Netherlands

[2]Utrecht University, Institute for Marine and Atmospheric Research, Princetonplein 5, 3584 CC Utrecht, the Netherlands

*Corresponding author: +31 15 2788147, k.m.simon@tudelft.nl

Abstract

The long-term glacial isostatic adjustment (GIA) signal at present-day is constrained via joint inversion of GPS vertical land motion rates and GRACE gravity data for a region encompassing Scandinavia, northern Europe and the British Isles, and the Barents Sea. The best-fit model for the vertical motion signal has a χ^2 value of approximately 1 and a maximum posterior uncertainty of 0.3-0.4 mm/yr. An elastic correction is applied to the vertical land motion rates that accounts for present-day changes to terrestrial hydrology as well as recent mass changes of ice sheets and glaciered regions. Throughout the study area, mass losses from Greenland dominate the elastic vertical signal and combine to give an elastic correction of up to +0.5 mm/yr in central Scandinavia. Neglecting to use an elastic correction may thus introduce a small but persistent bias in model predictions of GIA vertical motion even in central Scandinavia where vertical motion is dominated by long-term GIA. The predicted gravity signal is generally less well-constrained than the vertical signal, in part due to uncertainties associated with the correction for contemporary ice mass loss in Svalbard and the Russian Arctic. The GRACE-derived gravity trend is corrected for present-day ice mass loss using estimates derived from the ICESat and CryoSat missions, although a difference in magnitude between GRACE-inferred and altimetry-inferred regional mass loss rates suggests the possibility of a non-negligible GIA response here either from millennial-scale or Little Ice Age GIA.

Solid Earth Discuss., https://doi.org/10.5194/se-2018-8
Manuscript under review for journal Solid Earth
Discussion started: 7 February 2018

1. Introduction

Long-term glacial isostatic adjustment (GIA) is the process by which the Earth's solid surface and underlying mantle deform in response to loading by the large ice sheets that existed during the last glaciation. Because the time-scale of Earth's viscoelastic relaxation is up to several thousand years, ongoing GIA is usually the dominant present-day deformation signal in formerly glaciated areas that are tectonically quiescent (for example, up to 1 cm/yr land uplift around the northwestern Gulf of Bothnia). Outside formerly glaciated regions, the GIA signal often remains large enough to form a significant component of observed present-day deformation and sea-level change rates. Constraint of the long-term GIA signal at present-day is therefore required for accurate separation of the paleo and the more recent contributions to present-day land deformation and gravity change. This problem is complicated further by the fact that the GIA signal itself is temporally and spatially complex, and poorly constrained by models designed to describe both ice cover during the last glaciation and the structure of the Earth.

This paper constrains the long-term GIA signal in Scandinavia and northern Europe through the simultaneous inversion of vertical land motion rates from GPS and gravity change rates from GRACE. Corresponding uncertainties are also empirically estimated for the preferred model(s). Forward GIA model predictions typically have no formal uncertainty estimation although parameter variation suggests that forward model uncertainty is large. The estimation of formal model uncertainty is therefore a notable advantage of semi-empirical or data-driven methodologies. Similar empirical and semi-empirical approaches have been implemented to estimate regional long-term GIA signals in Antarctica (Riva et al. 2009, Gunter et al. 2014), North America (Sasgen et al. 2012, Simon et al. 2017), Alaska (Jin et al. 2016) and Fennoscandia (Hill et al. 2010, Zhao et al. 2012). Here, our methodology is based on that of Hill et al. (2010); relative to their previous work, we update both the GPS and GRACE datasets, expand the study area to include northern Europe and the British Isles to the south and the Barents Sea to the north, and incorporate a second model of ice sheet history into the *a priori* input. There are three main goals: i) to model the paleo GIA signal at present-day in a continuous region between Scandinavia and the British Isles, ii) to estimate empirically the uncertainty

Solid Earth Discuss., https://doi.org/10.5194/se-2018-8
Manuscript under review for journal Solid Earth
Discussion started: 7 February 2018

of the modelled signal, and iii) to assess the importance of applying an elastic correction to the vertical land motion data.

2. Model Inputs and Method

2.1 GPS Data

Rates of vertical land motion measured by GPS are taken from both Kierulf et al. (2014) and the Nevada Geodetic Laboratory (Blewitt et al. 2016) (**Figure 1**). The Kierulf et al. (2014) dataset has relatively dense coverage within the region of the former load centre of the Fennoscandian Ice Sheet (FIS), particularly in Norway, but sparse coverage elsewhere. The data from Blewitt et al. (2016) are thus used in the region outside the former ice sheet margin. In total, there are 459 stations. The data span the years 1996-2016; the time series length varies station to station from 3-20 years, with an average time series length of approximately 10 years.

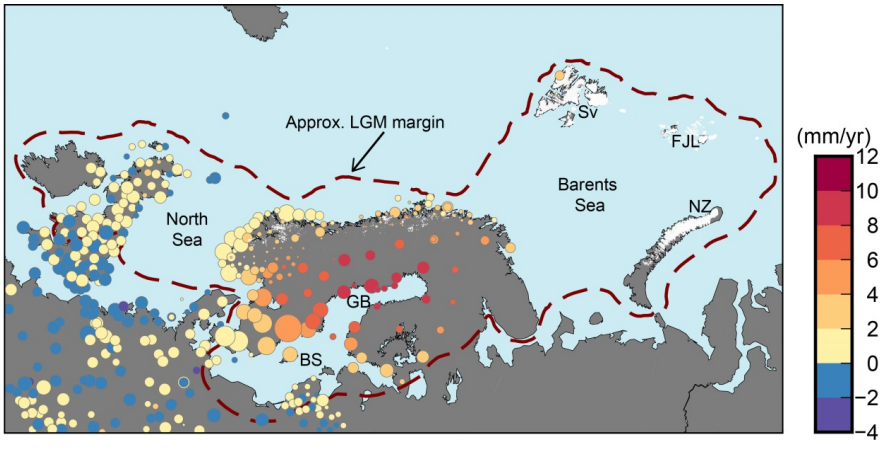

Figure 1. Rates of vertical land motion (mm/yr) for the GPS data used in the inversion, after correction for elastic effects (Section 2.3). BS – Baltic Sea, FJL – Franz Josef Land, GB – Gulf of Bothnia, NZ – Novaya Zemlya, Sv – Svalbard, FJL and NZ = Russian Arctic. Dark red dashed line shows the approximate boundary of ice cover at the Last Glacial Maximum (LGM). The size of the circles is inversely proportional to the measurement uncertainty.

As further described in Kierulf et al. (2014), their rates were derived using the GAMIT/GLOBK GPS analysis software (Herring et al. 2011), while the data from the Nevada Geodetic Laboratory were calculated using the MIDAS trend estimator, an algorithm designed for automatic step detection in

Solid Earth Discuss., https://doi.org/10.5194/se-2018-8
Manuscript under review for journal Solid Earth
Discussion started: 7 February 2018

time series (Blewitt et al. 2016). Although the processing technique differs for each dataset, the two datasets are combined in order to achieve the best possible spatial coverage in the study area. Common sites in the two datasets compare within the observational uncertainties at all but one of thirty-one sites, and no apparent bias is observed between the differences at the shared sites. Because the uncertainties are consistently larger for the data from the Nevada Geodetic Laboratory than for the data from Kierulf et al. (2014), we use the common sites to determine an average uncertainty scaling factor (~2.25) to apply to the uncertainties in the latter dataset. The scaling avoids significantly biasing the inversion result towards fitting either dataset. Both datasets are aligned in the International Terrestrial Reference Frame 2008 (Altamimi et al. 2011), which is consistent with the CM frame to within ~0.2 mm/yr. As described in Section 2.3, an elastic correction is applied that accounts for recent changes in ice sheet and glacier volumes and terrestrial hydrology.

2.2 GRACE

The GRACE data are processed as in Simon et al. (2017). Rates of gravity change for a 10.5 year period from 2004.02-2014.06 are estimated using 113 GRACE Release-05 (RL05) monthly solutions from the University of Texas at Austin Center for Space Research (CSR). The coefficients are truncated at degree and order 96 (consistent with a spatial resolution of ~200 km). Values estimated from Satellite Laser Ranging (Cheng et al. 2013) replace the C_{20} coefficients. Following Klees et al. (2008), the monthly fields are filtered with a statistically optimal Wiener filter. The optimal filter incorporates the full variance-covariance information of the monthly solutions, and less aggressively filters in regions where signal is stronger. A mass trend is estimated that accounts for bias, annual, and semi-annual variations (**Figure 2**). The signal uncertainty is represented by the full variance-covariance matrix of the trend. Corrections for changes in the terrestrial hydrology cycle and ice mass loss from Svalbard and the Russian Arctic are applied as described in Section 2.3.

Solid Earth Discuss., https://doi.org/10.5194/se-2018-8
Manuscript under review for journal Solid Earth
Discussion started: 7 February 2018

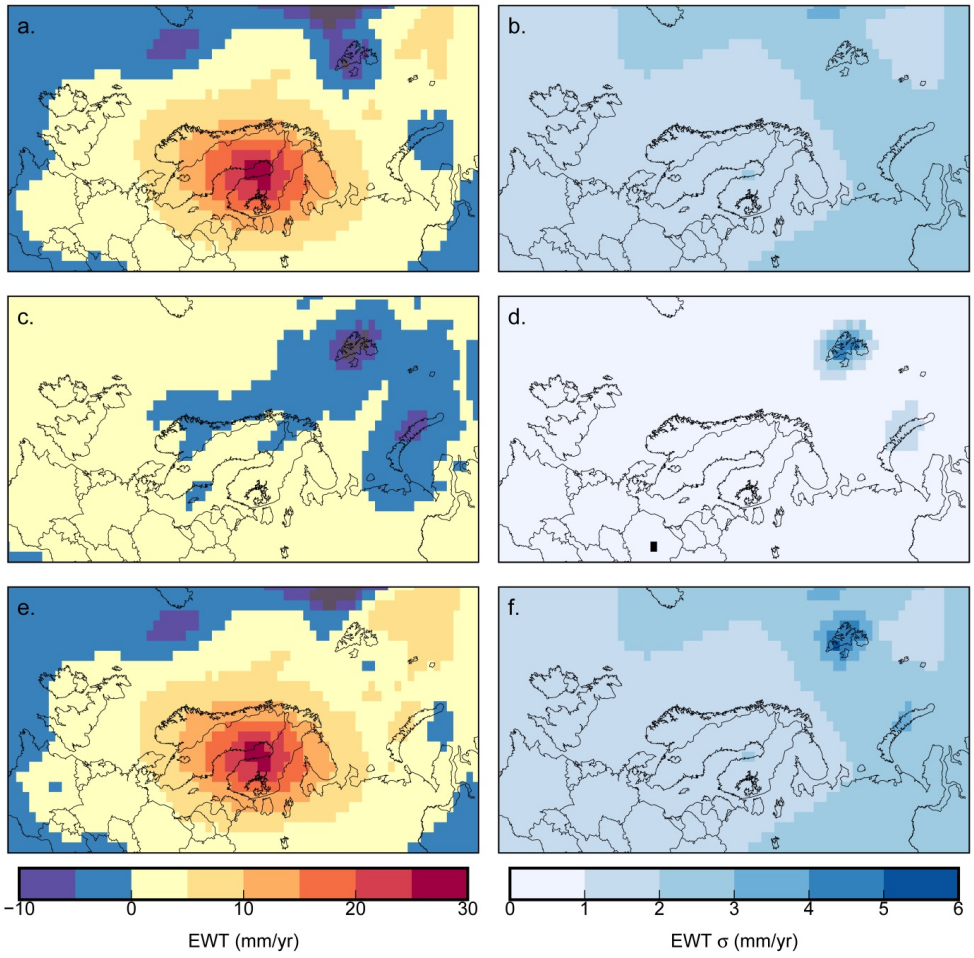

Figure 2. (a) Total gravity change rates measured from GRACE, (c) correction for terrestrial hydrology changes and present-day ice mass loss (Section 2.3), and (e) final corrected rates. (b,d,f) Same as (a,c,e) but rates are the 2σ uncertainties associated with the signal. Units are mm/yr change in equivalent water thickness (EWT).

2.3 Corrections for Terrestrial Hydrology and Present-day Ice Melt

Changes in terrestrial hydrology as well as present-day ice mass loss from Greenland, and glaciers and ice caps in Svalbard, the Russian Arctic, and Scandinavia may form a significant contribution to the total measured gravity change and vertical motion rates within the study area.

Solid Earth Discuss., https://doi.org/10.5194/se-2018-8
Manuscript under review for journal Solid Earth
Discussion started: 7 February 2018

GRACE

In the continental region and south of approximately 71.5° N latitude, hydrological changes are estimated with the model PCR-GLOBWB (Wada et al. 2014), which includes changes from anthropogenic groundwater depletion and dam retention. The trend is computed for 2004-2014 from 11 annual means on a 2° × 2° grid, consistent with the resolution of the GRACE data (**Figure 2c**). In glaciered regions (Scandinavia, Svalbard and the Russian Arctic), the hydrology model is not used to correct the input rates. Rather, it is assumed that present-day estimates of regional ice melt derived from altimetry observations should more accurately capture the dominant hydrological signals that would be modelled by PCR-GLOBWB.

Estimates of present-day mass changes in Scandinavia, the Russian Arctic, and Svalbard are summarized in **Table 1**, and vary considerably depending on estimation method and time period. Mass loss in Scandinavia is consistently small and generally estimated to be between -1.2 to -2 Gt/yr. Here, we apply a mass loss rate of -1.3 Gt/yr, determined by glaciological modelling (Marzeion et al. 2012, 2015).

In the Russian Arctic, glaciological estimates of mass change are consistent within uncertainties for the different time periods and suggest mass change between -21.0 to -24.7 Gt/yr. These rates are approximately twice those estimated by the ICESat and CryoSat missions, which estimate mass changes in this region of between -10.5 to -14.9 Gt/yr, with a small acceleration observed after 2010 (Wouters, *pers. comm.*, 2016). The smallest net mass change estimate for the Russian Arctic comes from GRACE, with -5.7 Gt/yr mass change observed between 2003-2013 (Schrama et al. 2014).

In Svalbard, estimated mass change rates are more discrepant. Again, glaciological estimates are the largest, but two estimates of -42.0 Gt/yr and -17.0 Gt/yr between 2003-2009 are not consistent within uncertainties and differ in magnitude by more than a factor of 2. Laser and radar altimetry estimates are smaller, and suggest a clear acceleration in mass loss since 2010 (-4.6 Gt/yr between 2003-2009

Solid Earth Discuss., https://doi.org/10.5194/se-2018-8
Manuscript under review for journal Solid Earth
Discussion started: 7 February 2018

141 and -16.5 Gt/yr between 2010-2014, Wouters, *pers. comm.*, 2016). As with the Russian Arctic,
142 GRACE is the estimation technique that records the smallest net mass change, with -4.0 Gt/yr
143 estimated in Svalbard between 2003-2013 (Schrama et al. 2014).

144

Study/Source	Svalbard (Gt/yr)	Russian Arctic (Gt/yr)	Scandinavia (Gt/yr)
2003-2009			
Marzeion et al. (2012, 2015) *(2003-2009)*	-42.0 ± 3.2 (gl)	-22.9 ± 4.7 (gl)	-1.2 ± 0.2 (gl)
Gardner et al. (2013) *(2003-2009)*	-17.0 ± 6.0 (gl) -5.0 ± 2.0 (I, G)	-21.0 ± 13.0 (gl) -11.0 ± 4.0 (I, G)	-2.0 ± 0.0 (gl)
Wouters (2016) *(2003-2009)*	-4.6 ± 1.2 (I)	-10.5 ± 1.3 (I)	-
2010-2014			
Wouters (2016) *(2010-2014)*	-16.5 ± 1.6 (C)	-14.9 ± 1.2 (C)	-
≥10 years time period			
Marzeion et al. (2012, 2015) *(2004-2013)*	-39.8 ± 2.2 (gl)	-24.7 ± 3.0 (gl)	-1.3 ± 0.1 (gl)
Average Wouters (2016) *(2003-2014)*	-10.6 ± 2.0 (I, C)	-12.7 ± 1.8 (I, C)	-
Schrama et al. (2014) *(2003-2013)*	-4.0 ± 0.7 (G)	-5.7 ± 0.9 (G)	+1.3 ± 0.9 (G)
This study	-10.6 ± 2.0 (I, C)	-12.7 ± 1.8 (I, C)	-1.3 ± 0.1 (gl)
This study, with scaling	-2.7 ± 2.0 (I, C)	-2.5 ± 1.8 (I, C)	-1.3 ± 0.1 (gl)*

145 **Table 1.** Estimates of present-day mass change for Svalbard, the Russian Arctic, and Scandinavia for
146 different time periods and from different sources. Letters in parentheses indicate estimation method; gl
147 - glaciological, I - IceSat, G - GRACE, C - CryoSat. All rates are in Gt/yr. *Not scaled.

148

149 The differing mass change estimates among measurement techniques for the Russian Arctic and
150 Svalbard raise the question of which value to use when applying a correction to the total GRACE trend
151 shown in **Figure 2a**. GRACE measures total mass changes (solid Earth plus cryosphere), while
152 glaciological and altimetry methods more accurately isolate changes to the cryosphere. Relative to

Solid Earth Discuss., https://doi.org/10.5194/se-2018-8
Manuscript under review for journal Solid Earth
Discussion started: 7 February 2018

GRACE, the latter two methods both consistently infer larger mass losses, suggesting that GRACE may contain a significant mass gain signal from the solid Earth, either from glacial isostatic adjustment from the last glaciation, or from the Little Ice Age (LIA). For both Svalbard and the Russian Arctic, we choose to apply an estimate that averages the ICESat and CryoSat estimates over the years 2003-2014 (**Table 1**). Subtracting these averaged rates from the total GRACE estimates for a similar time period (2003-2013, Schrama et al. 2014, **Table 1**), infers a reasonably consistent total solid Earth or GIA signal of +6.6-7 Gt/yr in the region.

However, applying the averaged ice melt corrections to Svalbard and the Russian Arctic creates a large mass gain signal over these two areas and a relatively smaller signal in the central Barents Sea; this pattern is generally inconsistent with ice coverage in the Barents Sea region suggested by several different Pleistocene ice sheet reconstructions (Auriac et al. 2016), and therefore inconsistent with the paleo GIA signal that the input signal should represent. Possible explanations for this inconsistency are: i) models of LGM ice cover in the region require thicker ice over Svalbard and the Russian Arctic than in the Barents Sea, ii) there is a large Little Ice Age GIA signal over these two regions, and/or iii) the Wiener filter applied to the GRACE data too aggressively filters signal in these small regions. The first explanation is unlikely because glacial margin chronology suggests that Svalbard and the Russian Arctic were located on or near the margin of the Barents Ice Sheet where ice cover would have been thinnest. To counteract the effect of either of the latter two explanations (LIA rebound or signal loss in GRACE), we apply ad-hoc scaling factors of 0.25 and 0.2 to the ice mass loss estimates in Svalbard and the Russian Arctic (**Table 1**), so that their removal from the total GRACE signal results in a spatial pattern in the residual (i.e., paleo GIA) signal that is approximately consistent with thicker LGM ice cover over the Barents Sea than around its margins (**Figure 2e**). Such a scaling factor approach is certainly not ideal, but serves to provide a GRACE input signal in the Barents Sea region that has a spatial pattern broadly consistent with expectations of the paleo GIA response to loading and unloading from the Barents Ice Sheet.

Solid Earth Discuss., https://doi.org/10.5194/se-2018-8
Manuscript under review for journal Solid Earth
Discussion started: 7 February 2018

GPS

Vertical land motion rates may likewise be affected by present-day ice mass loss and the terrestrial hydrology cycle. As with the GRACE data, the GPS data are corrected for changes to terrestrial hydrology south of 71.5° N latitude using predictions from the PCR-GLOBWB model, although here, the hydrology trend has been estimated from 1993-2014 to be more consistent with the length of the GPS time series. North of 71.5° N latitude, the same scaled corrections derived from ICESat and CryoSat are applied for present-day ice mass changes in Svalbard and the Russian Arctic. Throughout the study area, the GPS measurements are also corrected for additional elastic vertical motion from mass loss of the Greenland Ice Sheet, the Antarctic Ice Sheet and glaciers and ice caps in northern Canada. Mass loss of the Greenland Ice Sheet is estimated from 1993-2014 using surface mass balance estimates from RACMO2.3 (Noël et al. 2015) and ice discharge with a constant acceleration of 6.6 Gt/yr^2 (van den Broeke et al. 2016). Mass loss of the Antarctic Ice Sheet is also estimated from 1993-2014 assuming a constant acceleration in ice discharge of 2 Gt/yr^2. The scenarios for both Greenland and Antarctica are consistent with the mass balance estimates from Shepherd et al. (2012). For the Canadian Arctic, a constant mass loss rate of 60 Gt/yr is used (Gardner et al. 2013). All signals combine to yield a total net uplift of approximately 0.2-0.5 mm/yr throughout most of the study area, with Greenland mass loss providing the largest contribution (**Figure 3**). The additional uncertainties are also computed and added in quadrature to the measurement uncertainties; correction of the GPS data for non-GIA signals adds < ±0.05 mm/yr uncertainty in most of the study area and ~±0.1 mm/yr in Svalbard (**Figure 3**).

Finally, in addition to present-day ice mass loss signals, a correction of 4.33 ± 0.40 mm/yr is removed from the vertical motion rates for the two GPS sites on Svalbard (NYAL and LYRS). This value is an average of 3 scenarios from Mémin et al. (2014) which estimate the vertical land motion at Ny-Ålesund due to Pleistocene and Little Ice Age GIA signals; their estimates range from 3.31-4.95 mm/yr; thus the averaged correction of 4.33 mm/yr that is applied assumes that the signal from Pleistocene GIA is small and that most residual land motion here is from LIA rebound. After correction for present-day ice mass changes and approximated LIA uplift, the residual (inferred paleo GIA) vertical uplift rates at NYAL and LYRS are 2.64 ± 0.80 and 1.10 ± 2.64 mm/yr, respectively.

Solid Earth Discuss., https://doi.org/10.5194/se-2018-8
Manuscript under review for journal Solid Earth
Discussion started: 7 February 2018

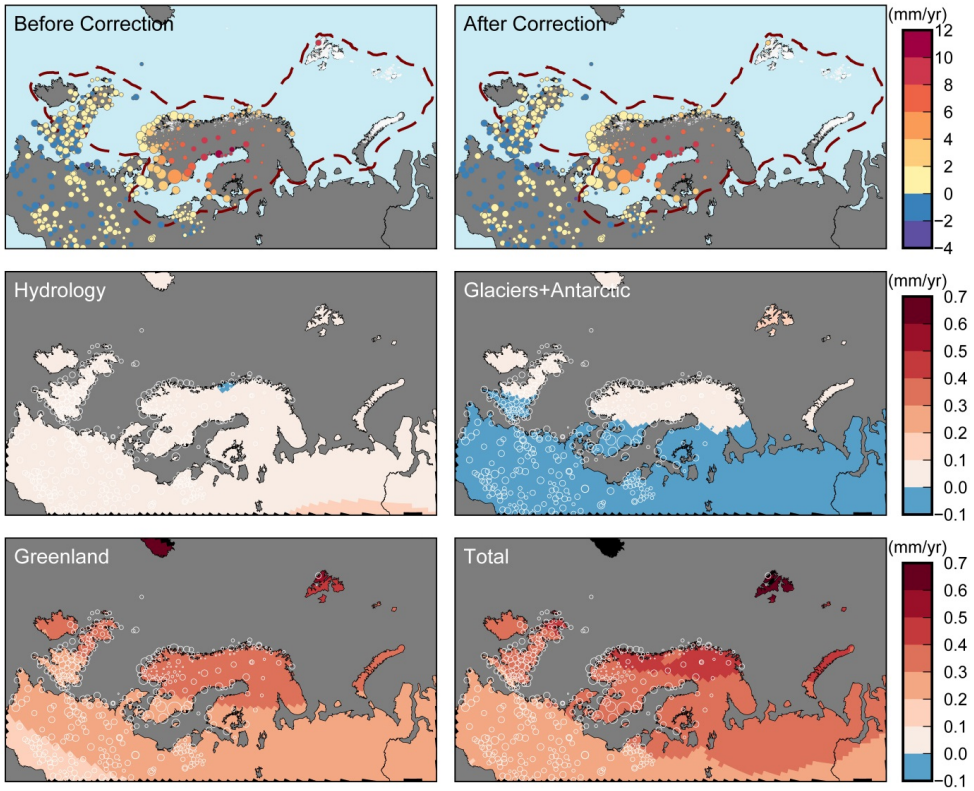

Figure 3. GPS-measured rates of vertical land motion before and after the applied elastic correction (top left and right). An elastic correction is computed for mass loss changes from Greenland, the West Antarctic Ice Sheet (WAIS), glaciers and ice caps in northern Canada, Svalbard and the Russian Arctic, and loading from the terrestrial hydrology cycle. Sites on Svalbard are additionally corrected for LIA uplift as discussed in the text.

2.4 *A Priori* Model Information

The prior model covariance matrix contains predictions from a set of forward GIA models that varies ice sheet history and mantle viscosity and is constructed as described in Hill et al. (2010) and Simon et al. (2017). Here, two different ice sheet histories are coupled to a suite of three-layer Earth models with an elastic lithosphere and varying upper and lower mantle viscosities.

The first ice sheet model is the global ICE-5G model (Peltier 2004). In the second ice sheet model, the glacial history over Fennoscandia and the British Isles is described by the model(s) from the Australian National University (ANU, Lambeck et al. 2010). This second version of the ice sheet model contains

Solid Earth Discuss., https://doi.org/10.5194/se-2018-8
Manuscript under review for journal Solid Earth
Discussion started: 7 February 2018

ICE-5G coverage over Greenland and Antarctica and the model of North American coverage presented in Simon et al. (2015, 2016). Tests indicate that varying the ice sheet history over North America has little impact on the predictions in Fennoscandia, although this variation is useful for studies that wish to expand the study area outside of the current study area. Relative to ICE-5G, LGM ice cover in the ANU model is thinner over the Barents Sea, thicker over Svalbard and Scotland, and discontinuous between Scandinavia and the British Isles (**Figure 4**).

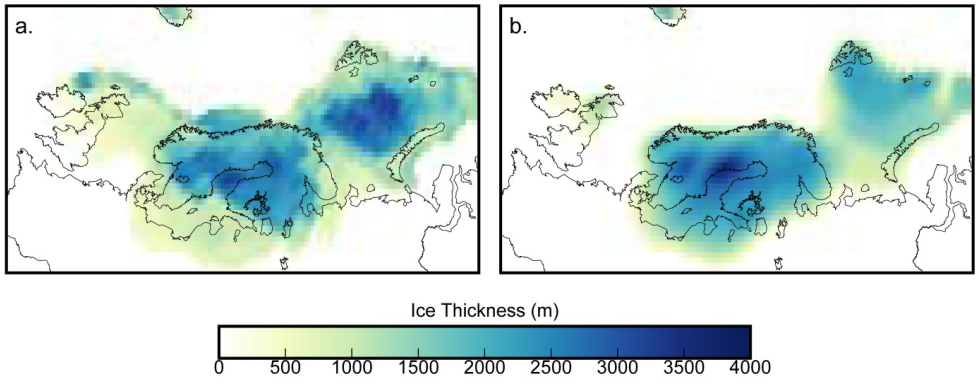

Figure 4. Last glacial maximum (LGM) ice cover in Scandinavia, the Barents Sea and the British Isles from ICE-5G (a) and the ANU model (b).

The Earth models have a 90 km thick elastic lithosphere and the upper and lower mantle viscosities span 0.2 – 2 × 10^{21} Pa s and 1 – 60 × 10^{21} Pa s, respectively. These viscosities span a range of plausible values in the upper and lower mantle. We note however that both the ICE-5G and ANU ice sheet models have been fit to a particular viscosity profile. While the coupling of differing Earth models to a 'tuned' ice sheet history may introduce artificially high variances, this concern may be countered by considering that the variances in such an *a priori* Earth-ice model set could almost certainly be made larger if any combination of 3D Earth structure, non-linear mantle rheology or glaciological and climatological constraints were additionally incorporated. A full covariance matrix is generated that relates the variances of each model prediction relative to the suite's average. All models are represented at spherical harmonic degree and order 256. The average response and uncertainties of the *a priori* set is shown in **Figure 5**.

Solid Earth Discuss., https://doi.org/10.5194/se-2018-8
Manuscript under review for journal Solid Earth
Discussion started: 7 February 2018

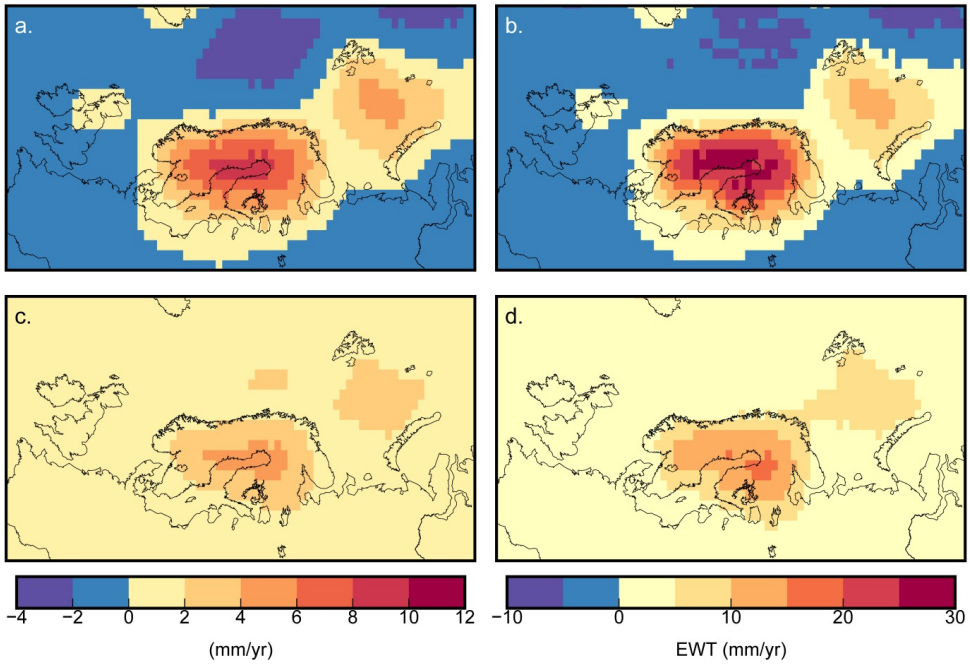

Figure 5. Averaged *a priori* rates of the Earth-ice model set. (a, c) Vertical rates and uncertainties. (b, d) Gravity change rates and uncertainties in units of equivalent water thickness (EWT) change.

2.5 Method

The least-squares adjustment method is based on the methodology of Hill et al. (2010) and extended by Simon et al. (2017). The method simultaneously inverts the data constraints (GPS, GRACE or both) with the *a priori* GIA model information and minimizes the misfit to both input types. As in Simon et al. (2017), variance component estimation (VCE) is also used to weight the input uncertainties. The prior models are combined with the data in three scenarios: inversion with the GPS data alone (D1), inversion with the GRACE data alone (D2), and inversion with both datasets (D3).

3. Results and Discussion

3.1 Prediction of Vertical Motion and Gravity Change

Vertical Motion

Solid Earth Discuss., https://doi.org/10.5194/se-2018-8
Manuscript under review for journal Solid Earth
Discussion started: 7 February 2018

The predicted GIA response and uncertainties for the D1-D3 scenarios are shown for vertical land motion (**Figure 6**). The incorporation of the GPS data in scenarios D1 and D3 leads to a similar pattern of regional uplift although relative to D1, the D3 scenario predicts slightly lower rates of uplift over the northern British Isles and in the Barents Sea. D1 and D3 have respective peak uplift rates of 9.8 and 9.2 mm/yr. When only the gravity data are inverted in the D2 scenario, the region of uplift is broader and the peak uplift rate is smaller at 7.1 mm/yr. In all cases, the peak uplift is centred over the northwestern region of the Gulf of Bothnia. The peak (1σ) uncertainty rates are ±0.36, ±0.43 and ±0.28 mm/yr for the D1-D3 cases. Similar to the results of Simon et al. (2017), the predicted uncertainties are largest where the signal is largest (around the Gulf of Bothnia) and/or the data coverage is sparsest and most poorly constrained (around the Barents Sea). In Finland, for example, the relatively large signal and the relatively sparse data coverage combine to create a region of larger uncertainty than in surrounding areas. The inclusion of VCE does not significantly impact the signal prediction but in general somewhat increases the estimation of posterior model uncertainty; the weighting factors determined by VCE are shown in **Table 2**.

Gravity Change

The predicted gravity change rates for D1-D3 are comparable to the predicted vertical motion rates in both the spatial pattern and relative magnitude (not shown). The peak mass change rates are again centred over the northern Gulf of Bothnia, and are 33.7, 24.3, and 32.3 mm/yr of equivalent water thickness change for the D1-D3 scenarios. The peak associated 1σ uncertainties are ±1.59, ±1.59 and ±1.22 mm/yr EWT.

Solid Earth Discuss., https://doi.org/10.5194/se-2018-8
Manuscript under review for journal Solid Earth
Discussion started: 7 February 2018

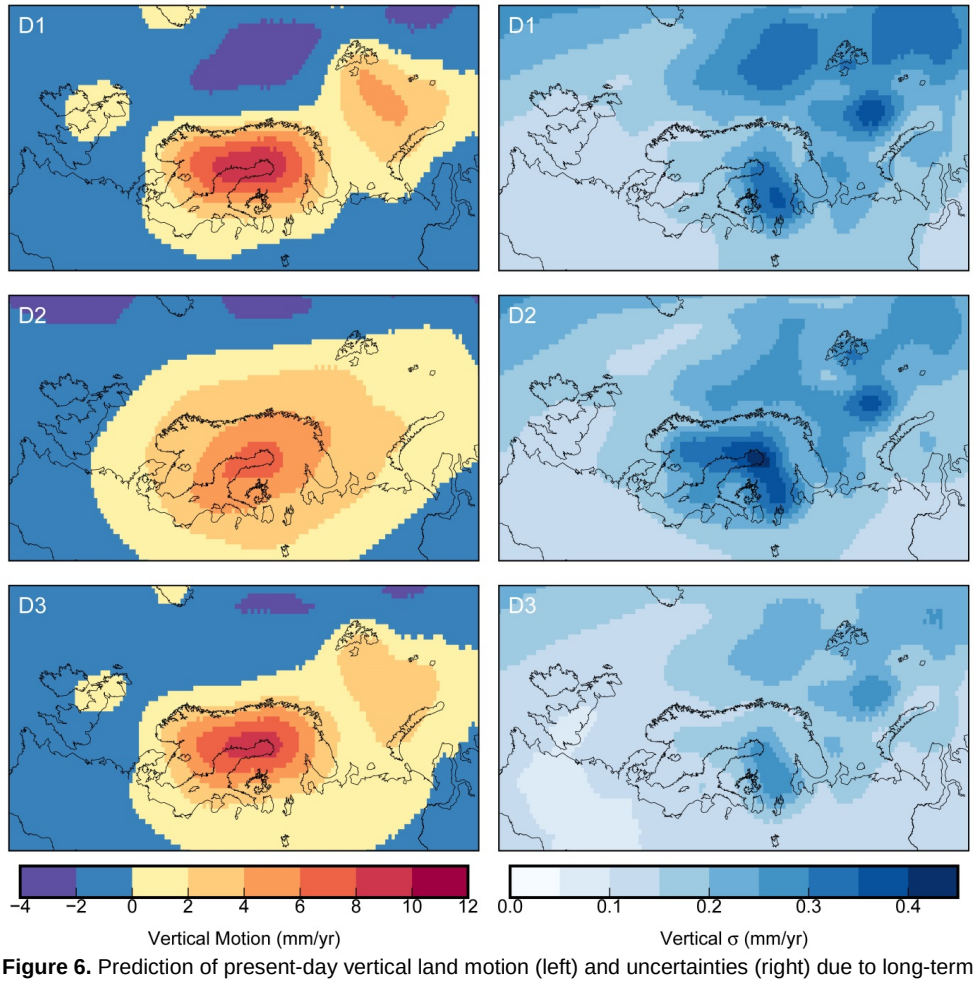

Figure 6. Prediction of present-day vertical land motion (left) and uncertainties (right) due to long-term GIA for the D1-D3 scenarios.

Data Incorporated	σ^2 Squared Value			Ratios	
	σ_1^2 (Vertical)	σ_2^2 (Gravity)	σ_μ^2 (Prior)	σ_1^2/σ_2^2	σ_1^2/σ_μ^2, σ_2^2/σ_μ^2
D1: Vertical only	0.85	-	0.94	-	0.92, -
D2: Gravity only	-	13.51	0.61	-	-, 22.02
D3: Vertical+Gravity	1.02	20.55	0.64	0.05	1.60, 32.29

Table 2. Results of the variance component analysis. $\sigma_1^2$and σ_2^2 are the variance factors applied to the vertical motion data (dataset 1) and gravity change data (dataset 2), respectively, and σ_μ^2 is the variance factor applied to the prior information. The ratios describe how each input is weighted relative to the other(s).

Solid Earth Discuss., https://doi.org/10.5194/se-2018-8
Manuscript under review for journal Solid Earth
Discussion started: 7 February 2018

294 3.2 Misfit Values and Residuals

295 For both χ^2 and RMS values, the D1 model provides the best fit to the vertical data, the D2 model
296 provides the best fit to the gravity data, and the D3 model provides the best fit overall (**Figure 7**). The
297 χ^2 values of the vertical prediction for both D1 and D3 are approximately equal to 1. The χ^2 values for
298 the gravity data are relatively large with the smallest value of 15.9 obtained for the D2 model. Scaling
299 the gravity data uncertainties by the VCE-determined scaling factors in **Table 2** reduces the overall χ^2
300 values for the gravity prediction to approximately 1.2 for the D2 and D3 models. However, the
301 statistical fit of the models to the gravity data remains generally worse than the fit to the vertical motion
302 data.

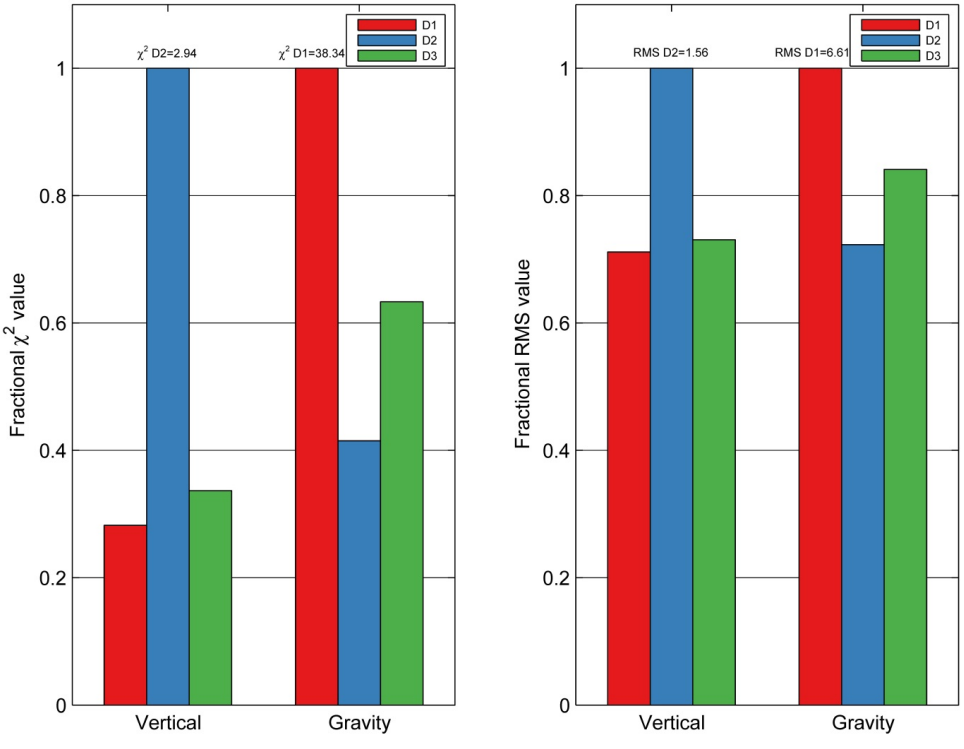

303

304 **Figure 7.** Fractional χ^2 and RMS values for each of the D1-D3 models. Fractional values are
305 determined relative to the value of the worst fitting model for both the vertical motion and gravity
306 change predictions (i.e., fractional χ^2 values of the vertical motion prediction are relative to D2 for
307 which $\chi^2 = 2.94$). χ^2 values are not VCE-scaled; see **Figure 8** for all χ^2 values including with and
308 without VCE scaling, where applicable.

309

Solid Earth Discuss., https://doi.org/10.5194/se-2018-8
Manuscript under review for journal Solid Earth
Discussion started: 7 February 2018

310 **Figures 8-9** summarize the spatial residuals for the best-fit D3 model and the binned residuals for all
311 models. The vertical motion residuals are unbiased and generally small. Regionally, the D3 model
312 underpredicts vertical motion in Scotland and conversely overpredicts vertical motion along parts of
313 the southern Norwegian coast and the Netherlands. The gravity residuals for D3 are relatively low for
314 much of the study area, although there is noticeable overprediction in central Scandinavia and in the
315 Barents Sea.

316

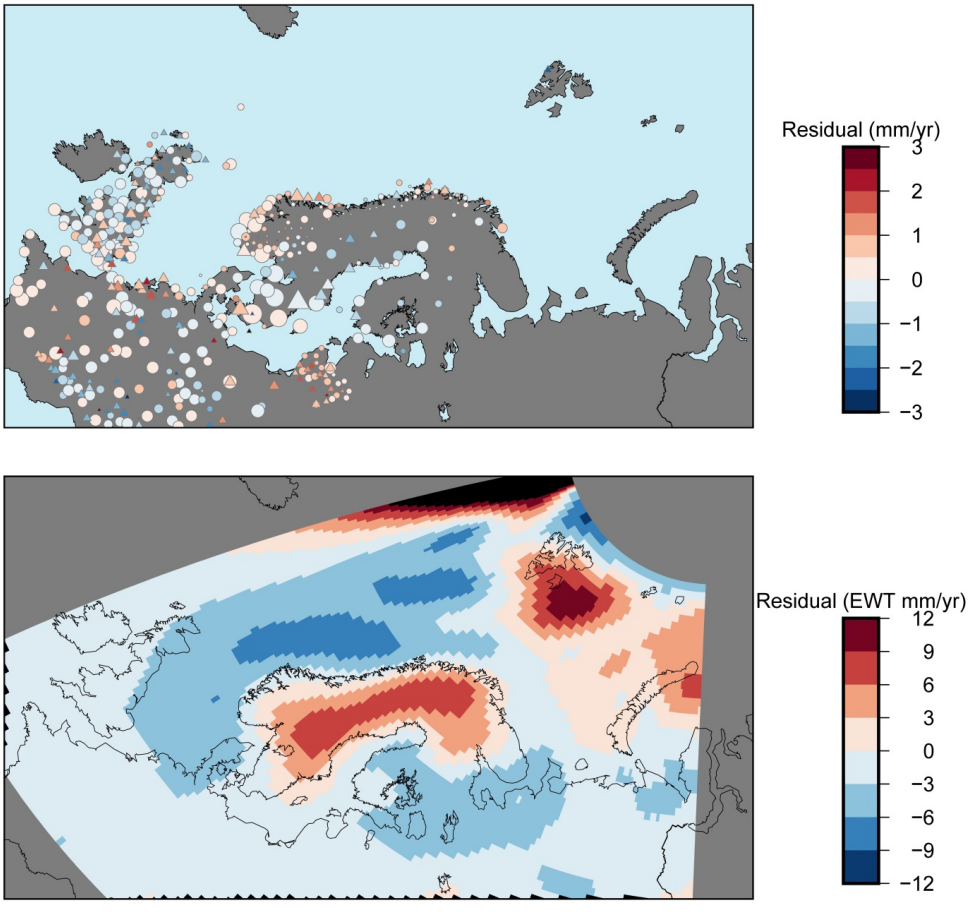

317

318 **Figure 8.** Spatial residuals for the D3 model for vertical motion (top) and gravity change (bottom). In
319 top panel, triangles indicate model prediction is outside the 1σ uncertainty of the measurement, circles
320 indicate model prediction is inside the 1σ uncertainty of the measurement.

321

Solid Earth Discuss., https://doi.org/10.5194/se-2018-8
Manuscript under review for journal Solid Earth
Discussion started: 7 February 2018

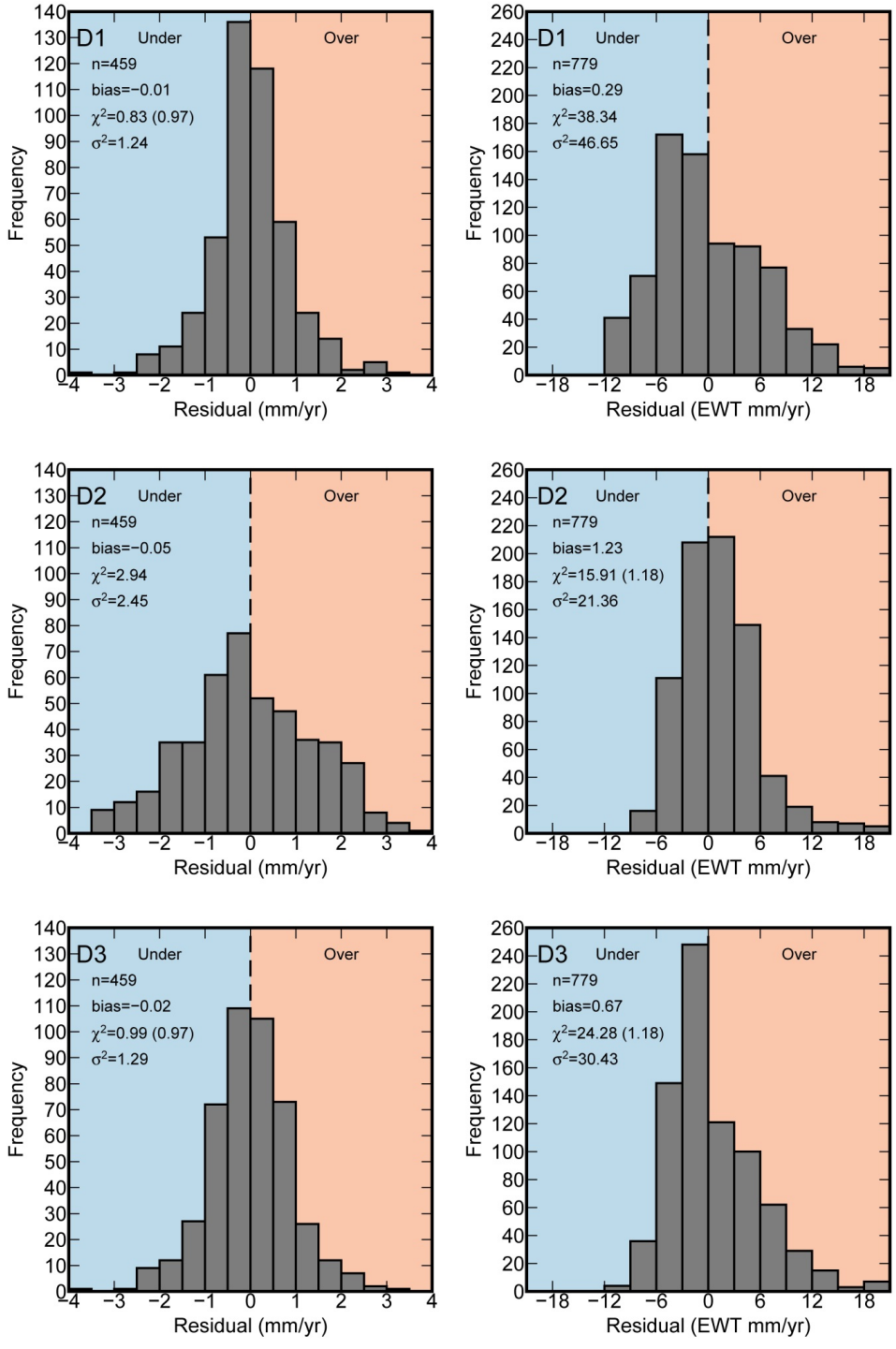

322

Solid Earth Discuss., https://doi.org/10.5194/se-2018-8
Manuscript under review for journal Solid Earth
Discussion started: 7 February 2018

Figure 9. Histogram of residuals for models D1-D3, for prediction of vertical motion (left) and gravity change (right). Pink and blue shading indicate model overprediction and underprediction, respectively. Where given, χ^2 values in brackets show the VCE-scaled χ^2 value.

3.3 Comparison of Vertical Motion Prediction to Other Models

We compare the vertical motion prediction of D1 to two other models that estimate the long-term GIA signal at present-day. The first model is the semi-empirical land uplift model NKG2016LU (Vestøl et al. 2016) designed by several researchers in collaboration with the Nordic Geodetic Commission (NKG). This model is constrained with GPS-measured vertical land motion rates updated from the dataset of Kierulf et al. (2014), levelling measurements and GIA model predictions. The second model is the forward GIA model ICE-6G (Peltier et al. 2015) which is constrained by a global dataset of vertical land motion measurements. The majority of the these data are GPS measurements from the global solution of JPL; within the study area of Scandinavia and northern Europe, additional measurements come from the BIFROST GPS network as well as a small number of SLR, DORIS and VLBI measurements (Argus et al. 2014, Peltier et al. 2015).

Figure 10 compares the vertical land motion predictions of D1, NKG2016LU, and ICE-6G. All comparisons are made relative to the vertical motion dataset presented in this paper, although as stated above, both NKG2016LU and ICE-6G were constrained with different variants of regional vertical land motion data. As well, NKG2016LU predictions are available on a smaller grid centred over Scandinavia, thus, we limit our comparison with this model to within these bounds (reducing the comparison dataset from 459 to 280 sites).

With no significant bias and a χ^2 value of less than 1, the D1 model provides a good fit to the data. As with the D3 model, the D1 model underpredicts vertical motion over the northern British Isles, and appears also to overpredict vertical motion around the Netherlands. The NKG2016LU model has a χ^2 value of less than 1 and a bias towards overprediction of 0.13 mm/yr. The overall bias towards overprediction is small, but is persistent particularly over Scandinavia (**Figure 10**). For the region north

Solid Earth Discuss., https://doi.org/10.5194/se-2018-8
Manuscript under review for journal Solid Earth
Discussion started: 7 February 2018

of 55°N (so approximately Scandinavia, 185 sites), the bias of the NKG2016LU model increases to 0.42 mm/yr. This bias is most likely attributable to the elastic correction applied to our GPS dataset, which is approximately +0.2-0.5 mm/yr over Scandinavia (**Figure 3**). Without an elastic correction applied to the GPS data, the NKG2016LU model has a bias of only -0.06 mm/yr in the region north of 55°N. The ICE-6G model underpredicts vertical motion at several sites in Scandinavia and has an overall χ^2 value of 1.33, somewhat higher than that of either D1 or NKG2016LU. At station NYAL on Svalbard, both the D1 and ICE-6G models underpredict vertical motion by more than 2 mm/yr, even after the applied corrections for present-day mass loss and possible LIA uplift. That the statistical fit to the data of both D1 and NKG2016LU is slightly better than the fit of the ICE-6G forward model is expected due to the fundamental difference in model type: unlike ICE-6G, both of the semi-empirical models explicitly incorporate the data into the prediction via formal inversion. Conversely, an advantage of ICE-6G and other models of its type is the direct insight they offer into the space-time evolution of the ice sheets, which cannot be inferred from a present-day empirical prediction alone.

Solid Earth Discuss., https://doi.org/10.5194/se-2018-8
Manuscript under review for journal Solid Earth
Discussion started: 7 February 2018

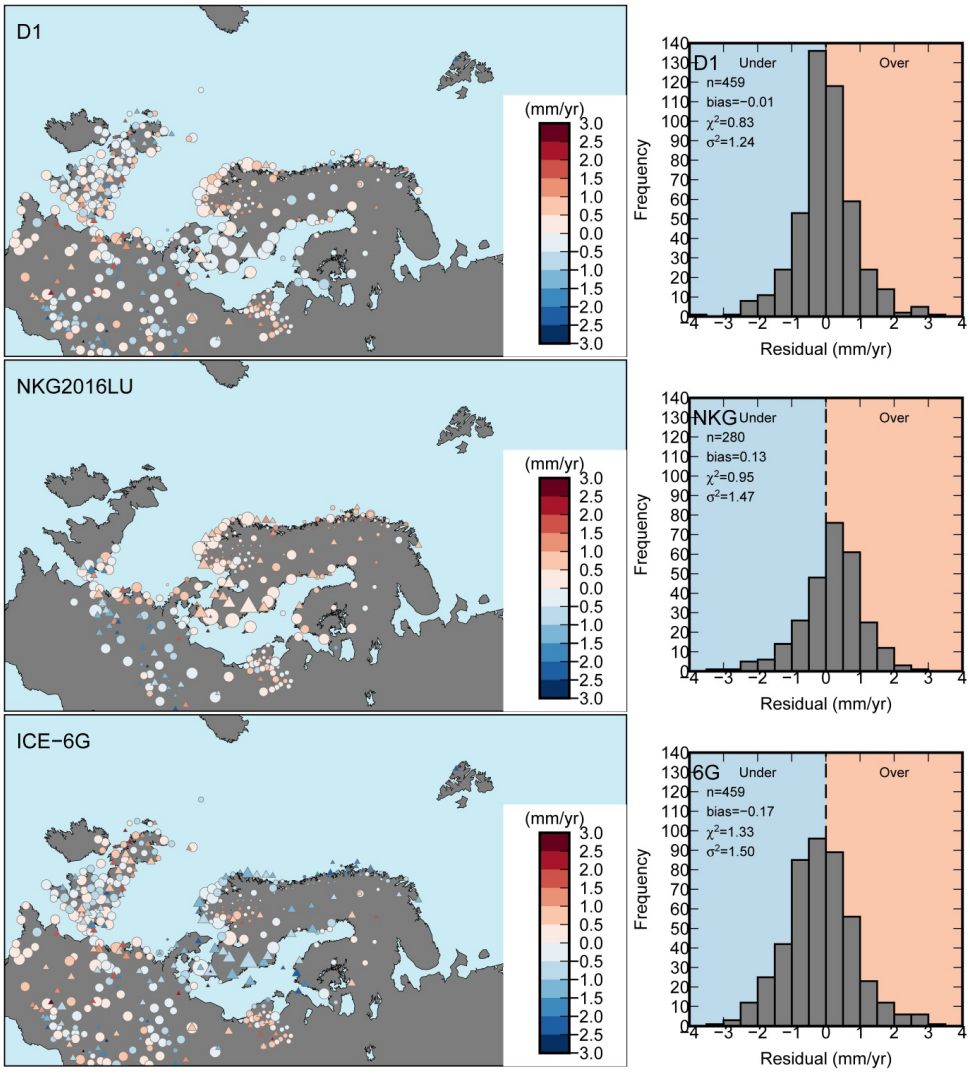

Figure 10. Spatial (left) and binned (right) vertical motion residuals for the D1, NKG2016LU and ICE-6G models (the latter two are abbreviated 'NKG' and '6G' in right-hand plots). Triangles indicate model prediction is outside the 1σ uncertainty of the measurement, circles indicate model prediction is inside the 1σ uncertainty of the measurement.

3.4 Tide Gauge Comparison

To assess the effect of GIA on regional sea-level change, we remove model D1's predictions of long-term GIA from mean sea-level trends at 17 tide gauge sites along the coast of the North Sea (**Figure 11**). The mean trends are taken from Frederikse et al. (2016a) who developed a state-space model to

Solid Earth Discuss., https://doi.org/10.5194/se-2018-8
Manuscript under review for journal Solid Earth
Discussion started: 7 February 2018

compute time-varying trends in tide gauge records, thereby taking into account unexplained (multi-) decadal variability. The rates shown here are averaged time-varying trends from Model C of Frederikse et al. (2016a), which removes decadal variability from the tide gauge time series using a hydrodynamic model developed to predict storm surge heights along the North Sea coast.

When corrected for the long-term GIA trends, which are assumed to be linear over decadal time-scales, the standard deviation of the trends decreases somewhat from 1.08 mm/yr to 0.89 mm/yr. The GIA correction is small at most sites, and at all sites except 10 and 11 (Hirtshals and Tregde), the averaged sea-level trends appear dominated by processes other than long-term GIA (**Figure 11**). At Hirtshals and Tregde, which are located nearest to the centre of the former FIS, the predicted GIA-induced sea-level trend is more than twice the magnitude of the averaged sea-level trend and removing the GIA signal shifts the original trend at these locations closer to the mean of the 17 locations. Regionally, the average GIA model trend is ~-0.4 mm/yr for the North Sea which is larger in magnitude than the GIA trend of ~0 mm/yr in the North Sea sea-level analysis of Frederikse et al. (2016b); this difference may in part be due to the influence of the ANU ice sheet model in the prior model, which predicts stronger subsidence over the North Sea than ICE-5G.

Removal of the GIA signal from all 17 locations increases the North Sea mean sea-level trend from 1.31 mm/yr to 1.58 mm/yr The GIA-corrected rates at 4 sites along the British Isles coastline (12, 13, 14 and 16) fall outside the standard deviation of the mean corrected rate. In the northern British Isles, around sites 13 and 14 (Wick and Aberdeen), model D1 underpredicts the magnitude of vertical motion and thus also the magnitude of relative sea-level change. However, even if the magnitude of RSL fall were larger in this region by up to 0.5 mm/yr, the GIA-corrected sea-level rates at Wick and Aberdeen would remain outside the standard deviation of the mean. At station Wick, the sea-level trend is particularly variable and non-linear at decadal scales (Frederikse et al. 2016a), suggesting that one averaged time-varying rate cannot be expected to adequately describe sea-level variation at this location. At any rate, such variability is insensitive to application of the relatively small and linear GIA correction for this region and it appears unlikely that the variability in sea-level trends along the

Solid Earth Discuss., https://doi.org/10.5194/se-2018-8
Manuscript under review for journal Solid Earth
Discussion started: 7 February 2018

British coast can be explained by GIA-induced sea-level change. Conversely, the variability in sea-level trends in the northeast North Sea, near the former FIS, is easily attributed to GIA.

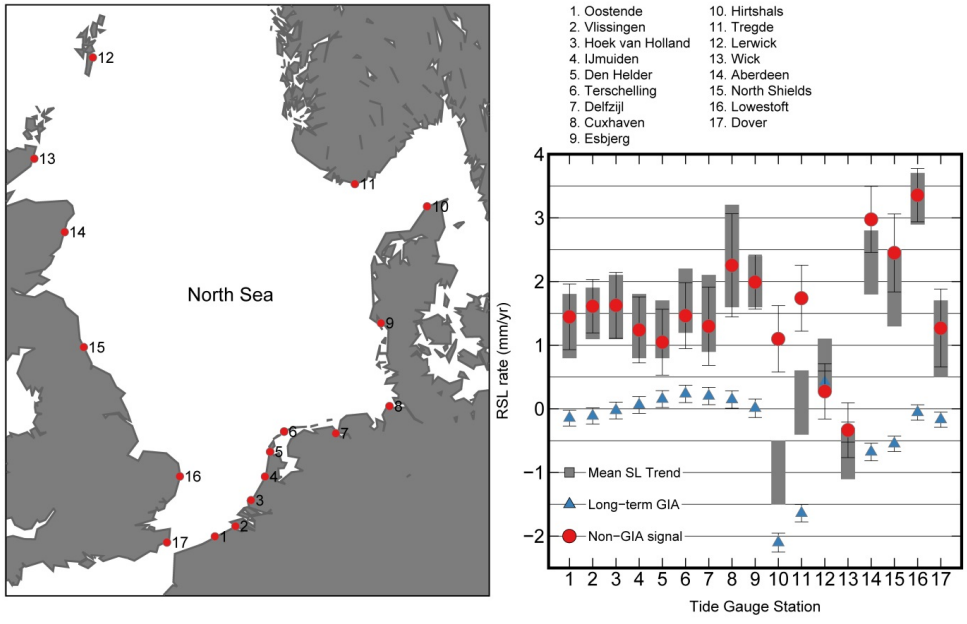

Figure 11. Comparison of mean total, long-term GIA and non-GIA sea-level trends (grey boxes, blue triangles, red circles) for 17 tide gauge stations in the North Sea. Long-term GIA trends are from model D1, mean sea-level trends are from Model C of Frederikse et al. (2016a).

4. Conclusion

We generate a data-driven prediction of the long-term GIA response at present-day in Scandinavia, northern Europe and the Barents Sea through the simultaneous inversion of GPS-measured vertical motion rates, GRACE-measured gravity change rates, and *a priori* GIA model information. In models D1-D3, we predict GIA motions for the inversion of the vertical motion data, the gravity data, and both datasets. In both the χ^2 and RMS sense, the vertical motion data alone have the poorest ability to predict gravity change, and vice versa. Predictions of the D3 model provide the best overall fit to both datasets.

In general, prediction of the gravity signal is problematic, with larger χ^2 values than those obtained for the vertical motion prediction. The poorer prediction of gravity change is in part due to the uncertainty of the present-day mass loss effect in the Barents Sea region. The mass loss signal estimated by GRACE over Svalbard and the Russian Arctic is significantly smaller than estimates obtained from satellite altimetry. This difference may be the result of signal loss in the GRACE data from application of the Wiener filter or may also indicate that there is a non-zero component of ongoing glacial isostatic adjustment from the LIA.

The vertical motion signal is overall better predicted than the gravity signal. Both the D1 and D3 models have χ^2 values of ≤ 1 and predict rates of vertical motion that are within the 1σ uncertainty of the observations throughout most of the study area. Regions of misfit persist in Scotland and around the Netherlands, where the model underpredicts and overpredicts rates of vertical motion, respectively. The misfit in Scotland may be partly due to both positive and negative rates of vertical motion that are present in the data over relatively short distances. Further analysis and filtering of the GPS dataset may be useful in this region. In the Netherlands, Kooi et al. (1998) found that present-day subsidence from sediment compaction as well as tectonic movements may contribute significantly to vertical land motion; correction for these effects may serve to reduce some of the misfit in this region.

The prediction of vertical land motion has a small but non-negligible sensitivity to the application of an elastic correction. The elastic correction applied in this study is between 0.2-0.5 mm/yr; the largest contribution comes from mass loss of the Greenland Ice Sheet which yields regional uplift with a southeastward decreasing gradient. When the model predictions from another semi-empirical model of GIA vertical motion, NKG2016LU, are compared to the corrected GPS data, a small but uniform bias of +0.42 mm/yr is present in the model predictions over Scandinavia. Conversely, when D1 model predictions generated with the corrected data are compared to the uncorrected data from the same region, a uniform bias of -0.35 mm/yr is present, consistent with expectations. Both NKG2016LU and D1 (and D3) have vertical motion χ^2 values ≤ 1 over their respective study areas. However, while the magnitude of the bias is smaller than the observational uncertainty on many of the measurements, it is generally larger than the estimated posterior model uncertainty. Also, because only anthropogenic

Solid Earth Discuss., https://doi.org/10.5194/se-2018-8
Manuscript under review for journal Solid Earth
Discussion started: 7 February 2018

448 hydrological signals (and not natural hydrological signals) were included in the elastic correction, it is
449 likely that the applied elastic correction is conservative in this region.

450

451 Therefore, the presence of such a bias in the vertical motion prediction suggests that while long-term
452 GIA is the dominant contributor to vertical motion in central Scandinavia, that it is still worthwhile to
453 correct GPS land motion rates for present-day elastic signals, so long as these signals are adequately
454 approximated (e.g., Riva et al. 2017). This conclusion however highlights a fundamental assumption
455 that underpins the data-driven methodology: that the input data can be adequately 'cleaned' for
456 processes not arising from long-term GIA. Even with applied corrections for hydrology and
457 contemporary ice mass loss, this assumption may not always be adequate, especially in regions
458 where model misfits relative to the data are spatially coherent. Thus, the success of data-driven GIA
459 predictions are evaluated by two criteria: i) the estimation of realistic posterior uncertainties that are
460 smaller than those associated with *a priori* knowledge and measurement uncertainty, and ii) the ability
461 of the final model to provide a good fit to the data. The vertical motion predictions of models D1 and
462 D3 satisfy both criteria for most of the study area and thus can provide a useful tool with which to
463 separate long-term GIA signals from shorter-term forcing.

464

465

466

467

468

Solid Earth Discuss., https://doi.org/10.5194/se-2018-8
Manuscript under review for journal Solid Earth
Discussion started: 7 February 2018

469 **Acknowledgements**

470 We would like to thank Anthony Purcell for providing the ANU ice sheet model for Europe and the
471 British Isles, Yoshihide Wada for making the PCR-GLOBWB hydrology model available, and Bert
472 Wouters for providing altimetry estimates of recent mass loss for Svalbard and the Russian Arctic.
473 This work is part of the project for a Multi-Scale Sea-Level model (MuSSeL), funded by the
474 Netherlands Organization for Scientific Research, VIDI Grant No. 864.12.012.

Solid Earth Discuss., https://doi.org/10.5194/se-2018-8
Manuscript under review for journal Solid Earth
Discussion started: 7 February 2018

475 **References**

476 Altamimi, Z., Collilieux, X., and Métivier, L., 2011. ITRF2008: an improved solution of the international
477 terrestrial reference frame. Journal of Geodesy 85, 457–473, doi:10.1007/s00190-011-0444-
478 4.

479 Argus, D.F., Peltier, W.R., Drummond, R., and Moore, A.W., 2014. The Antarctica component of
480 postglacial rebound model ICE-6G_C (VM5a) based on GPS positioning, exposure age
481 dating of ice thicknesses, and relative sea level histories. Geophysical Journal International
482 198, 537–563, doi:10.1093/gji/ggu140.

483 Auriac. A., Whitehouse, P.L., Bentley, M.J., Patton, H., Lloyd, J.M., and Hubbard, A., 2016. Glacial
484 isostatic adjustment associated with the Barents Sea ice sheet: A modelling inter-
485 comparison. Quaternary Science Reviews, 147, 122-135,
486 doi:10.1016/j.quascirev.2016.02.011.
487
488 Blewitt, G., Kreemer, C., Hammond, W.C., and Gazeaux, J., 2016. MIDAS robust trend estimator for
489 accurate GPS station velocities without step detection. Journal of Geophysical Research -
490 Solid Earth 121, doi:10.1002/2015JB012552.

491 Cheng, M.K., Tapley, B.D., and Ries, J.C., 2013. Deceleration in the Earth's oblateness. Journal of
492 Geophysical Research 118, 740-747, doi:10.1002/jgrb.50058.
493
494 Frederikse, T., Riva, R., Slobbe, C., Broerse, T., and Verlaan, M., 2016a. Estimating decadal
495 variability in sea level from tide gauge records: An application to the North Sea. Journal of
496 Geophysical Research 121, 1529–1545, doi:10.1002/2015JC011174.
497
498 Frederikse, T., Riva, R., Kleinherenbrink, M., Wada, Y., van den Broeke, M., and Marzeion, B., 2016b.
499 Closing the sea level budget on a regional scale: Trends and variability on the Northwestern
500 European continental shelf. Geophysical Research Letters 43, doi:10.1002/2016GL070750.
501
502 Gardner, A.S., Moholdt, G., Cogley, J.G., Wouters, B., Arendt, A.A., Wahr, J., Berthier, E., Hock, R.,
503 Pfeffer, W.T., Kaser, G., Ligtenberg, S.R.M., Bolch, T., Sharp, M.J., Hagen, J.O., van den
504 Broeke, M.R., and Paul, F., 2013. A reconciled estimate of glacier contributions to sea level
505 rise: 2003 to 2009. Science 340, 852-857, doi:10.1126/science.1234532.
506
507 Gunter, B.C., Didova, O., Riva, R.E.M., Ligtenberg, S.R.M., Lenaerts, J.T.M., King, M.A., van den
508 Broeke, M.R., and Urban, T., 2014. Empirical estimation of present-day Antarctic glacial
509 isostatic adjustment and ice mass change. The Cryosphere 8, 743–760, doi:10.5194/tc-8-
510 743-2014.
511
512 Herring, T., King, R., and McClusky, S., 2011. Introduction to GAMIT/GLOBK release 10.4, Technical
513 Report, Massachusetts Institute of Technology, Cambridge, USA.
514
515 Hill, E.M., Davis, J.L., Tamisiea, M.E., and Lidberg, M., 2010. Combination of geodetic observations
516 and models for glacial isostatic adjustment fields in Fennoscandia. Journal of Geophysical
517 Research 115, doi:10.1029/2009JB006967.

518 Jin, S., Zhang, T.Y., and Zou, F., 2016. Glacial density and GIA in Alaska estimated from ICESat,
519 GPS and GRACE measurements. Journal of Geophysical Research 122,
520 doi:10.1002/2016JF003926.
521
522 Kierulf, H.P., Steffen, H., Simpson, M.J.R., Lidberg, M., Wu, P., and Wang, H. 2014. A GPS velocity
523 field for Fennoscandia and a consistent comparison to glacial isostatic adjustment models.
524 Journal of Geophysical Research – Solid Earth 119, 6613–6629,
525 doi:10.1002/2013JB010889.

526 Klees, R., Revtova, E.A., Gunter, B.C., Ditmar, P., Oudman, E., Winsemius, H.C., and Savenije,
527 H.H.G., 2008. The design of an optimal filter for monthly GRACE gravity models.
528 Geophysical Journal International 175, 417–432, doi:10.1111/j.1365-246X.2008.03922.x.

Kooi, H., Johnston, P., Lambeck, K., Smither, C., Molendijk, R., 1998. Geological causes of recent (~100 yr) vertical land movement in the Netherlands. Tectonophysics 299, 297–316.

Lambeck, K., Purcell, A., Zhao, J. and Svensson, N.-O., 2010. The Scandinavian ice sheet: from MIS 4 to the end of the last glacial maximum, Boreas, 39, 410–435, doi:10.1111/j.1502-3885.2010.00140.x

Marzeion, B., Jarosch, A.H., and Hofer, M., 2012. Past and future sea-level change from the surface mass balance of glaciers. The Cryosphere 6, 1295–1322, doi:10.5194/tc-6-1295-2012.

Marzeion, B., Leclercq, P.W., Cogley, J.G., and Jarosch, A.H., 2015. Brief Communication: Global reconstructions of glacier mass change during the 20th century are consistent. The Cryosphere 9, 2399–2404, doi:10.5194/tc-9-2399-2015.

Mémin, A., Spada, G., Boy, J-.P., Rogister, Y., and Hinderer, J., 2014. Decadal geodetic variations in Ny-Ålesund (Svalbard): role of past and present ice-mass changes. Geophysical Journal International 198, 285-297, doi:10.1093/gji/ggu134.

Noël, B., van de Berg, W.J., van Meijgaard, E., Munneke, P.K., van de Wal, R.S.W., and van den Broeke, M.R., 2015. Evaluation of the updated regional climate model RACMO2.3: Summer snowfall impact on the Greenland Ice Sheet, Cryosphere 9, 1831–1844, doi:10.5194/tc-9-1831-2015.

Peltier, W.R., 2004. Global glacial isostasy and the surface of the ice-age Earth: The ICE-5G (VM2) model and GRACE. Annual Reviews of Earth and Planetary Sciences 32, 111–149, doi:10.1146/annurev.earth.32.082503.144359.

Peltier, W.R., Argus, D.F., and Drummond, R., 2015. Space geodesy constrains ice age terminal deglaciation: The global ICE-6G_C (VM5a) model. Journal of Geophysical Research 119, doi:10.1002/2014JB011176.

Riva, R.E.M., Gunter, B.C., Urban, T.J., Vermeersen, B.L.A., Lindenbergh, R.C., Helsen, M.M., Bamber, J.L., van de Wal, R.S.W., van den Broeke, M.R., and Schutz, B.E., 2009. Glacial isostatic adjustment over Antarctica from combined ICESat and GRACE satellite data. Earth and Planetary Science Letters 288 516–523, doi:10.1016/j.epsl.2009.10.013.

Riva, R.E.M., Frederikse, T., King, M.A., Marzeion, B., and van den Broeke, M.R., 2017. Brief Communication: The global signature of post-1900 land ice wastage on vertical land motion. The Cryosphere 11, 1327–1332, doi:10.5194/tc-11-1327-2017.

Sasgen, I., Klemann, V., and Martinec, Z., 2012. Towards the inversion of GRACE gravity fields for present-day ice-mass changes and glacial-isostatic adjustment in North America and Greenland. Journal of Geodynamics 59–60, 49–63, doi:10.1016/j.jog.2012.03.004.

Schrama, E.J.O., Wouters, B., and Rietbroek, R., 2014. A mascon approach to assess ice sheet and glacier mass balances and their uncertainties from GRACE data. Journal of Geophysical Research 119, 6048–6066, doi:10.1002/2013JB010923.

Shepherd, A. *et al.*, 2012. A reconciled estimate of ice-sheet mass balance, Science 338, 1183–1189, doi:10.1126/science.1228102.

Simon, K.M., James, T.S., and Dyke, A.S., 2015. A new glacial isostatic adjustment model of the Innuitian Ice Sheet, Arctic Canada. Quaternary Science Reviews 119, 11–21, doi:10.1016/j.quascirev.2015.04.007.

Simon, K.M., James, T.S., Henton, J.A., and Dyke, A.S., 2016. A glacial isostatic adjustment model for the central and northern Laurentide Ice Sheet based on relative sea-level and GPS measurements. Geophysical Journal International, 205, 1618-1636, doi:10.1093/gji/ggw103.

588 Simon, K.M., Riva, R.E.M., Kleinherenbrink, M., and Tangdamrongsub, N., 2017. A data-driven model
589 for constraint of present-day glacial isostatic adjustment in North America. Earth and
590 Planetary Science Letters, 474: 322-333, doi:10.1016/j.epsl.2017.06.046.

591 van den Broeke, M. R., Enderlin, E.M., Howat, I.M., Munneke, P.K., Noël, B.P.Y., van de Berg, W.J.,
592 van Meijgaard, E., and Wouters, B., 2016. On the recent contribution of the Greenland ice
593 sheet to sea level change, Cryosphere 10, 1933–1946, doi:10.5194/tc-10-1933-2016.
594
595 Vestøl, O., Ågren, J., Steffen, H., Kierulf, H., Lidberg, M., Oja, T., Rüdja, A., Kall, T., Saaranen, V.,
596 Engsager, K., Jepsen, C., Liepins, I., Paršeliūnas, E., and Tarasov, L., 2016. NKG2016LU,
597 an improved postglacial land uplift model over the Nordic-Baltic region. Nordic Geodetic
598 Commission (NKG) Working Group of Geoid and Height Systems.

599 Wada, Y., Wisser, D., and Bierkens, M.F.P., 2014. Global modeling of withdrawal, allocation and
600 consumptive use of surface water and groundwater resources. Earth System Dynamics 5,
601 15–40, doi:10.5194/esd-5-15-2014.
602
603 Wouters, B., 2016. Personal communication.
604
605 Zhao, S., Lambeck, K., and Lidberg, M., 2012. Lithosphere thickness and mantle viscosity inverted
606 from GPS-derived deformation rates in Fennoscandia. Geophysical Journal International
607 190, 278-292, doi:10.1111/j.1365-246X.2012.05454.x.